HHS Public Access

Author manuscript

Neuroimage. Author manuscript; available in PMC 2017 February 01.

Published in final edited form as:

Neuroimage. 2016 February 1; 126: 219–228. doi:10.1016/j.neuroimage.2015.11.042.

Quantitative β mapping for calibrated fMRI

Christina Y. Shu[1], **Basavaraju G. Sanganahalli**[2], **Daniel Coman**[2], **Peter Herman**[2], **Douglas L. Rothman**[1,2], and **Fahmeed Hyder**[1,2]

[1]Department of Biomedical Engineering, Yale University, New Haven, CT, USA

[2]Department of Radiology and Biomedical Imaging and Magnetic Resonance Research Center, Yale University, New Haven, CT, USA

Abstract

The metabolic and hemodynamic dependencies of the blood oxygenation level-dependent (BOLD) signal form the basis for calibrated fMRI, where the focus is on oxidative energy demanded by neural activity. An important part of calibrated fMRI is the power-law relationship between the BOLD signal and deoxyhemoglobin concentration, which in turn is related to the ratio between oxidative demand (CMR_{O2}) and blood flow (CBF). The power-law dependence between BOLD signal and deoxyhemoglobin concentration is signified by a scaling exponent β. Until recently [R1.1] most studies assumed a β value of 1.5, which is based on numerical simulations of the extravascular BOLD component. Since basal value of CMR_{O2} and CBF can vary from subject-to-subject and/or region-to-region, a method to independently measure β in vivo should improve the accuracy of calibrated fMRI results. We describe a new method for β mapping through characterizing R_2' - the most sensitive relaxation component of BOLD signal (i.e., the reversible magnetic susceptibility component that is predominantly of extravascular origin at high magnetic field) - as a function of intravascular magnetic susceptibility induced by an FDA-approved superparamagnetic contrast agent. In α-chloralose anesthetized rat brain, at 9.4T, we measured β values of ~0.8 uniformly across large neocortical swathes, with lower magnitude and more heterogeneity in subcortical areas. Comparison of β maps in rats anesthetized with medetomidine and α-chloralose revealed that β is independent of neural activity levels at these resting states. We anticipate this method for β mapping can help facilitate calibrated fMRI for clinical studies.

Keywords

blood volume; SPIO; feraheme; neurometabolic coupling; neurovascular coupling

Address correspondence and reprint requests to: Christina Y. Shu / D. S. Fahmeed Hyder, N143 TAC (MRRC), 300 Cedar Street, Yale University, New Haven, CT 06520, U.S.A. christina.shu@yale.edu / fahmeed.hyder@yale.edu, Tel: +1-203-785-6205, Fax: +1-203-785-6643.

AUTHOR CONTRIBUTIONS

CYS, DLR, and FH designed study; CYS, BGS, PH, FH conducted study; CYS, PH, DC, FH conducted data analysis; CYS, BGS, DC, PH, DLR, FH wrote the paper.

DISCLOSURE/CONFLICT OF INTEREST

The authors declare that there are no conflicts of interest.

1. INTRODUCTION

In fMRI studies the blood oxygenation level-dependent (BOLD) contrast originates from changes in transverse relaxation rate of tissue water, which is given by a power-law function of magnetic susceptibility induced by paramagnetic deoxyhemoglobin in the blood (Ogawa et al., 1993). The BOLD contrast from venous blood is most observable due to the nearly full hemoglobin saturation at the arterial input side. Because the deoxyhemoglobin concentration in venous blood indicates the coupling between cerebral blood flow (CBF), cerebral blood volume (CBV), and cerebral metabolic rate of oxygen consumption (CMR_{O2}), this power-law relationship governs the estimated value of CMR_{O2} in calibrated fMRI studies (Hoge et al., 1999; Hyder et al., 2001). In other words, when a localized brain region experiences altered neural activity, the evoked change in CMR_{O2} can be calculated based on simultaneously measured variations in BOLD, CBF, and CBV

$$\Delta BOLD/BOLD_0 = \mathrm{M}\left[1-\left(CMR_{O_2}/CMR_{O_{2,0}}\right)^{\beta}(CBF/CBF_0)^{-\beta}(CBV/CBV_0)\right] \quad (1)$$

where CBV is commonly converted from CBF measurements via Grubb's coefficient (Grubb et al., 1974), M is an echo time dependent constant whose value incorporates the resting hemodynamic and metabolic conditions of the subject, and the parameters with and without subscripted “0” represent the basal and activated values, respectively.

To quantify CMR_{O2} change with **eq. (1)**, parameters like M and β are needed in addition to independent measurements of BOLD, CBV, and CBF (Hoge et al., 1999; Hyder et al., 2001). Although CBV is not directly measured in human studies, it can be measured in animal studies with exogenous superparamagnetic MRI contrast agents that primarily reside in the intravascular space (for recent reviews see (Kim et al., 2013; Wang, 2011)). M is a factor that reflects the dynamic range of the BOLD signal in a given voxel, whereas β is the scaling exponent that describes the BOLD signal's dependencies on the local deoxyhemoglobin acting as the endogenous paramagnetic agent in venous blood.

Various experimental methods to measure M have been described in the literature, where its behavior across magnetic field strengths, brain regions, and basal activity states has been explored (for a recent review see (Hyder et al., 2013b; Shu et al., 2015)). Since methods to measure β in vivo are limited, it is common to assume β as 1.5. This β value was determined on the basis of Monte Carlo simulations of the transverse relaxation rate of extravascular water as magnetization of water protons in between capillary vessels vary within a specific range (Boxerman et al., 1995; Davis et al., 1998; Kennan et al., 1994). To date, a β value of 1.5 is assumed in most calibrated fMRI studies (Ances et al., 2008; Kastrup et al., 1999; Restom et al., 2008; Stefanovic et al., 2004; Wey et al., 2011; Wu et al., 2002) amidst concern for CMR_{O2} calculation error caused by oversimplification of the β parameter (Buxton et al., 2004; Mohtasib et al., 2012). Given the importance of the β parameter for extracting fractional changes in CMR_{O2}, an experimental method to measure β is needed.

Previous studies suggested that the BOLD signal's relationship to paramagnetic deoxyhemoglobin in venous blood is affected by factors such as vessel size (Boxerman et

al., 1995; Ogawa et al., 1993), vessel geometry (Yablonskiy and Haacke, 1994), diffusion of water molecules through extravascular space (Buxton et al., 2004; Kennan et al., 1994), magnetic field strength (Boxerman et al., 1995; Duong et al., 2003), echo time of the experiment (Gati et al., 1997), and whether measurements are made with spin-echo or gradient-echo sequences (Kennan et al., 1994). The transverse relaxation component of BOLD signal that is most sensitive toward blood oxygenation is given by R_2' (see **Theory**), which represents the reversible magnetic susceptibility component and at high magnetic field (≥7T) it is primarily of extravascular origin (Donahue et al., 2011; Hoge et al., 1999; Hyder and Rothman, 2012; Silvennoinen et al., 2003). While it is difficult to separately measure all the factors that contribute to β in vivo, it is feasible to measure R_2' in vivo (Blockley et al., 2015; Fujita et al., 2003; Kida et al., 2000; Shu et al., 2015). In fact, β could be determined experimentally through analyzing the relationship between R_2' and susceptibility levels in blood.

Toward this end, we enhanced the intravascular magnetic susceptibility by sequentially increasing amount of superparamagnetic contrast agent in the blood. By measuring R_2' as a function of the contrast agent concentration, β was experimentally determined on a voxel-by-voxel basis. In line with the principles of calibrated fMRI, at 9.4T β measured by this approach reflects the extravascular component (see **Theory** and **Materials and Methods** for theoretical and experimental concepts). Additionally, we showed consistent results between Molday and Feraheme. Whereas Molday is used widely in animal studies, Feraheme has recently been applied in human fMRI studies as an efficient contrast agent for measuring CBV-weighted signal (Christen et al., 2013; Christen et al., 2014; D'Arceuil et al., 2013). Since the relationship between β and brain region or activity level was not hypothesized or tested previously, here we measured β values across different brain regions (in white and gray matter) and different brain states. Levels of neuronal firings and energy metabolism differ significantly for rats under α-chloralose or medetomidine, as is the case of human brain under different stages of wakefulness or disease. Comparing β with variation of anesthesia level in rats is thus analogous to comparing β in humans with variation of activity levels due to alertness or disease. Implications of the β results in the context of calibrated fMRI were also tested with simulations.

2. THEORY

The transverse relaxation rate measured in a spin-echo experiment (i.e., R_2) represents the blood oxygenation-dependent relaxation effect in the intermediate to fast diffusion regime (for definitions of the different diffusion regimes, please see (Kennan et al., 1994)), while the relaxation rate measured in a gradient-echo experiment (i.e., R_2*) embodies an additional relaxation effect that is due to variation in local magnetic susceptibility in the slow diffusion regime (i.e., R_2') (Kida et al., 2000). Under well-shimmed conditions, dephasing due to macroscopic field inhomogeneity can be ignored and therefore R_2* and R_2 can be described by

$$R_2^* = R_2'(Y) + R_2(Y) + R_2(0) \quad (2a)$$

$$R_2 = R_2(Y) + R_2(0) \quad (2b)$$

where Y is the O_2 saturation of hemoglobin, $R_2(0)$ is the relaxation assigned to non-susceptibility components, and $R_2'(Y)$ and $R_2(Y)$ are the reversible and non-reversible relaxation components weighted by susceptibility related to blood oxygenation level. Previously it was shown that both R_2^* (measured by a gradient-echo sequence) and R_2 (measured by a spin-echo sequence) values are impacted when hemoglobin saturation changes, where the former dominates (Kida et al., 2000). Thus, the absolute difference between the two measured rates gives

$$R_2' = R_2^* - R_2 \quad (3)$$

which is the reversible component captured only by a gradient-echo and is the most sensitive component of the BOLD signal with respect to blood oxygenation (Kida et al., 2000).

At high magnetic field the intravascular weighting of these measured rates is reduced (Donahue et al., 2011; Hyder et al., 2000a; Kennan et al., 1994; Kida et al., 2000; Silvennoinen et al., 2003), and thus susceptibility-sensitive portion of the extravascular BOLD signal can be obtained by measuring R_2' directly using **eq. (3)** (Kida et al., 2000). R_2' in vivo is a function of CBV and deoxyhemoglobin concentration (i.e., [dHb]) raised to the β exponent (Boxerman et al., 1995)

$$R_2' = A \cdot CBV \cdot [dHb]^{\beta} \quad (4)$$

where A is a proportionality constant whose value may change due to subject and/or experimental conditions (Hoge et al., 1999). Generalizing the magnetic susceptibility effects induced by endogenous and exogenous contrast agents (Kennan et al., 1994), when a superparamagnetic contrast agent is present the effective susceptibility in blood incorporates susceptibilities of both deoxyhemoglobin (χ_{dHb}) and the contrast agent (χ_m). Thus R_2' at rest can be expressed as

$$R_2' = A \cdot CBV \cdot \left(\left(\chi_{dHb} \cdot c_{dHB,0} + \chi_m \cdot c_{m,0}\right) \cdot B_0\right)^{\beta} \quad (5)$$

where c_m is the molar concentration of the agent, B_0 is static magnetic field strength, and $c_{dHB,0}$ and $c_{m,0}$ are initial concentrations of deoxyhemoglobin and contrast agent, respectively. Since A, CBV, and B_0 remain unchanged for the same subject at rest, the ratio between two measurements of R_2' at incremental doses of contrast agent is equivalent to

$$ln\left(R_2'/R_{2\,0}'\right) = \beta \; ln\left[\left(\chi_{dHb} \cdot c_{dHB} + \chi_m \cdot c_m\right) / \left(\chi_{dHb} \cdot c_{dHB,0} + \chi_m \cdot c_{m,0}\right)\right] \quad (6)$$

where index "0" represents the initial conditions. Because the susceptibility effect induced by the superparamagnetic contrast agent is much stronger than deoxyhemoglobin (i.e., $\chi_{dHb} \cdot c_{dHB} << \chi_m \cdot c_m$), **eq. (6)** can be simplified further to

$$ln\left(R_2'/R_{2\,0}'\right)=\beta\ ln\left(c_m/c_{m,0}\right) \quad (7)$$

where β is given by the slope of a linear relationship between $\ln(R_2'/R_{2\,0}')$ and $\ln(c_m/c_{m,0})$.

3. MATERIALS and METHODS

3.1 Animal preparation

All protocols were approved by Yale's Institutional Animal Care and Use Committee (IACUC) and all procedures followed the National Institute of Health *Guide for the Care and Use of Laboratory Animals*. Sprague-Dawley rats (male, ~300 g) were artificially ventilated (70% N_2O, 30% O_2) and normal physiology was maintained throughout the experiment. The rats were anesthetized with either α-chloralose (i.p. 80 mg/kg initial dose, then 40 mg/kg/hr; n = 8) or medetomidine hydrochloride (i.v. 0.1 mg/kg/hr; n = 6). A protocol designed by Pawela et al was adopted for infusing medetomidine hydrochloride (Pawela et al., 2009), and we doubled its infusion rate every two hours during the experiments. Blood pressure (90±6 mmHg), pH (7.4±0.1), and blood gases (pO_2 = 100±11 mmHg, pCO_2 = 37±3 mmHg) were examined regularly with a femoral arterial line.

3.2 Electrophysiology

Rats (anesthetized with α-chloralose (n = 3) and medetomidine (n = 3)) were positioned with a stereotaxic holder on a vibration-free table inside a Faraday cage. The forepaw (i.e., $S1_{FL}$) somatosensory regions (4.4 mm lateral and 1.0 mm anterior to Bregma) were drilled to create a tiny burr hole through which high-impedance tungsten microelectrodes (FHC Inc, Bowdoin, ME) were inserted. Neural signals were recorded with a micro 1401 A/D converter unit and Spike2 software (CED, Cambridge, UK). Band pass (300 – 3,000 Hz) and low pass (<150 Hz) filters were used to select multiunit activity (MUA) and local field potential (LFP) from the raw signals (Krohn-Hite Inc, Brockton, MA). Spike density function was calculated from the sorted spikes (extracted from MUA recordings) by convolving it with a 100 ms SD Gaussian kernel.

3.3 Image acquisition

The MRI data was obtained on a 9.4T system interfaced to a Direct Drive console (Agilent Tech, Santa Clara, CA) and an actively shielded gradient coil with 500 mT/m maximum gradient strength at 180 μs rise time (Magnex, UK). We used a custom-built ^1H quadrature surface radio-frequency (B_1) coil (3.5 cm diameter) and the static field inhomogeneity was optimized with second-order spherical harmonics shimming until the half-height line width of water across the regions from which voxels were analyzed was less than 15-20 Hz (Juchem et al., 2014). At the beginning of experiments, the B_1 power was optimized to reduce variation in 180° refocusing pulse for the spin-echo experiments. Prior to injecting contrast agents, multiple slices of R_2* and R_2 maps were acquired with spin-wrap two-dimensional-Fourier-Transform (2DFT) gradient-echo and spin-echo sequences, respectively, covering majority of the rat brain. The parameters used (gradient-echo/spin-echo) were: repetition time (TR) = 500/3000 ms, echo time (TE) = 5-40/10-100 ms, number of averages: 4/1, number of dummy scans: 16/8, slice thickness = 0.5mm, and field-of-view

(FOV) = 32×32 mm. Scan durations for R_2 and R_2* acquisitions were approximately 7 minutes and 4 minutes, respectively. The superparamagnetic contrast agents used were Feraheme (particle size 17-31 nm, AMAG Pharmaceuticals Inc., Cambridge, MA, USA) and Molday (particle size 30 nm, Molday, BioPAL Inc., Worcester, MA, USA). All rats received three intravenous bolus injections of Feraheme (incremental doses of 3.5 mg/kg) or Molday (incremental dose of 5 mg/kg). While Feraheme was studied with α-chloralose and medetomidine anesthesia, Molday was studied only with α-chloralose. Following each injection, multiple slices of R_2* and R_2 maps were acquired again.

3.4 Data processing

Data were processed off-line in MATLAB (MathWorks, Natick, MA, USA) and the Bioimage Suite (www.bioimagesuite.org) (Papademetris et al., 2006). The images were registered to a reference atlas (scalablebrainatlas.incf.org). Cerebral spinal fluid (CSF) and edge artifacts due to misregistration were removed. To ensure that susceptibility of contrast agent dominates the signal, amount of reduction in signal intensity with each dose injection was calculated relative to pre-injection. One-way analysis of variance (ANOVA) was used to test the tissue-dependence in signal intensity drop. R_2 and R_2* images were calculated from single exponential (and multi-exponential in one subject for comparison) decay fitting of gradient-echo and spin-echo intensities as a function of TE. R_2' images were calculated using **eq. (3)** and β maps were calculated using **eq. (7)**. Lower brain area near large vessels and ventricles were not included in analysis, as the efficacy of B_0 shimming was limited in these locations. An ROI template (Calabrese et al., 2013) was overlaid on β maps to calculate mean and standard deviation (SD) in 22 regions of interest (ROIs). The ROIs included: internal capsule (ic); septum (Spt); diagonal domain (DiagD); striatum (Str); diencephalon (Dien); hippocampal formation (Hif); pallidum (GP); accumbens (Acb); fimbria fornix (fi); preoptic area (POA); bed nuclei stria terminalis (BNST); corpus callosum (cc); olfactory structure (Olf); primary (V1) and secondary (V2) visual cortices; primary (M1) and secondary (M2) motor cortices; primary somatosensory cortices of fore limb ($S1_{FL}$), upper lip ($S1_{ULP}$), hind limb ($S1_{HL}$), and barrel field ($S1_{BF}$); secondary somatosensory cortex (S2). These ROIs were categorized into "white matter", "cortical gray matter", and "subcortical gray matter". Diencephalon covered both gray and white matter and therefore was not categorized. Kolmogorov-Smirnov test was used to confirm standard normal distribution of data in both groups of subjects for all ROI at the 5% significance level. One-way and Two-way analysis of variance (ANOVA) as well as Student's t-test were used to compare regional β-values under α-chloralose and medetomidine, with a 5% significance level.

3.5 Calibrated fMRI simulations

Simulations investigated the impact of β on accuracy of CMR_{O2} calculation. First, BOLD and CBF data (e.g., as in hypercapnia challenge for calibrated fMRI (Hoge, 2012)) were simulated for a fixed M value of 10% but different β values, for an isometabolic condition (i.e., $CMR_{O2}/CMR_{O2,0} = 1$ in **eq. (1)**)

$$\Delta BOLD/BOLD_0 = \mathrm{M}\left[1-(CBF/CBF_0)^{\alpha-\beta}\right] \quad (8)$$

where α is the Grubb's coefficient frequently assumed to be 0.38. (Grubb et al., 1974). $\Delta BOLD/BOLD_0$ was calculated with **eq. (8)** for different β values (ranging from 0.6 and 2.0) using five different levels of CBF/CBF_0 equally spaced between 1 and 1.4. The CBF range represented the range typically measured during gas challenges experiments in humans. These simulations were performed for α of 0.2 and 0.4. Then, impact of α, β, and M to the calculated $CMR_{O2}/CMR_{O2,0}$ during a somatosensory stimulation in rats were simulated based on (Hoge et al., 1999):

$$CMR_{O_2}/CMR_{O_{2,0}}=[1-(\Delta BOLD/BOLD_0)/\mathrm{M}]^{(1/\beta)}(CBF/CBF_0)^{(1-\alpha/\beta)} \quad (9)$$

Values of $\Delta BOLD/BOLD_0$ and CBF/CBF_0 were taken from previous high field rat and human studies (Donahue et al., 2011; Herman et al., 2013; Silva et al., 1999).

4. RESULTS

Physiological parameters such as blood pH, pCO_2, and pO_2 for all rats in each group were maintained within normal limits throughout the scans (**Table 1**). According to one-way ANOVA, there was no significant difference ($p>0.1$) in the degree of post-injection signal drop between gray and white matter (**Supplementary Figure 1**), and therefore we do not anticipate the contrast agent mechanism to be affected by tissue type. All results are shown as mean ± standard deviation (SD). Kolmogorov-Smirnov test confirmed normal distribution of data in both groups of subjects for all ROI at the 5% significance level, which suggests that our data are statistically significant.

4.1 Changes in R_2, R_2*, and R_2' in the whole brain with Feraheme

In α-chloralose anesthetized rats, the R_2, R_2*, and R_2' images measured prior to and after each dose of Feraheme (3.5 mg/kg) are shown in **Figure 1**. Prior to injection, for the whole brain R_2 was ~22 s^{-1}, R_2* was ~36 s^{-1}, and R_2' was ~14 s^{-1}. With each subsequent injected dose, all of these rates increased incrementally (i.e., per dose R_2 by ~0.6 s^{-1}, R_2* by ~10 s^{-1}, and R_2' by ~9 s^{-1}). As the changes in R_2 were much smaller compared to changes in R_2* and R_2', R_2* and R_2' were highly correlated to each other ($r^2 = 0.95$). The R_2 maps were quite homogeneous across different cortical layers, while the R_2* and R_2' were higher in superficial layers of cortex. Using **eq. (7)**, a whole brain β value of 0.7±0.1 was obtained with R_2'.

4.2 Comparison of R_2' changes: β values with Molday vs. Feraheme

Molday and Feraheme were individually injected into separate rats (anesthetized with α-chloralose) with incremental doses of 5 and 3.5 mg/kg body weight, respectively. After each injected dose, R_2' increased substantially for both agents. **Table 2** summarizes respective R_2' results for a few ROIs (e.g., $S1_{FL}$, cc, M1, S2, and Str). **Figure 2** shows the R_2' data from individual rats where β was fitted with **eq. (7)**. The β values with Feraheme ranged from 0.5 to 0.7 across these ROIs with a minimum in cc and the cortical ROIs ranged from 0.6 to 0.8. While the changes in R_2' were much larger with Molday, the slopes of fitting (i.e., β) were quite similar across regions. All correlation values (r^2) were higher than 0.92, reflecting strong linear relationships. Since Feraheme has been used in humans (Christen et

al., 2013; Christen et al., 2014; D'Arceuil et al., 2013), we chose this contrast agent to conduct detailed analysis of β across regions and states.

4.3 Variations of β across regions

Figure 3 shows multiple slices of R_2' measured at each Feraheme dose and β for the whole brain under α-chloralose. A uniform β among the cortical gray matter was measured, with a mean of 0.78±0.06. In the subcortical gray matter, β was lower in magnitude, with a mean of 0.61±0.06. The white matter regions had a mean of 0.56±0.07. According to the result of one-way ANOVA, there was no significant difference in β across the neocortical gray matter regions ($p>0.05$). The magnitudes of β were generally lower in the subcortical gray matter regions with greater extent of heterogeneity than found in the neocortex. Among all ROIs, the highest value of β was observed among $S1_{FL}$ (0.81±0.15), $S1_{ULP}$ (0.80±0.15), $S1_{HL}$ (0.80±0.17), and $S1_{BF}$ (0.81±0.15), whereas the lowest value of β was observed in ic (0.48±0.08).

4.4 Comparison of β across brain states

The neural activity and β maps measured in rats anesthetized with α-chloralose and medetomidine are summarized in **Figure 4**. The mean β values were significantly greater than the SD β values for both states (**Supplementary Figure 2**). The spike density functions for the medetomidine-anesthetized rats were approximately double compared to the α-chloralose-anesthetized rats (**Figure 4A**), and the root mean square (RMS) of LFP signals also exhibited a ~100% difference **(Table 3)**. β maps calculated from both groups showed similar patterns across brain regions (**Figure 4B**), while the corpus callosum was distinctively outlined by lower values. In terms of magnitude, in the whole brain β with medetomidine (β_{med} = 0.62±0.15) was similar to β with α-chloralose (β_{α} = 0.66±0.15). The two groups were not significantly different from each other as suggested by two-way ANOVA ($p>0.05$). Likewise, Student's t-test did not give significant difference in β for any individual ROI ($p>0.05$). Additionally, regions of highest β were found in nearly identical cortical locations. Similar to the results for α-chloralose in **Figure 3**, maximum β values were among the primary somatosensory cortical regions ($\beta_{med, S1FL}$ = 0.81±0.01, $\beta_{med, S1ULP}$ = 0.79±0.07, $\beta_{med, S1HL}$ = 0.84±0.06, $\beta_{med, S1BF}$ = 0.81±0.07), while minimum β values were found in ic ($\beta_{med, ic}$ = 0.43±0.01). Among subcortical gray matter regions maximum β value was observed in Hif in both groups ($\beta_{\alpha, Hif}$ = 0.73±0.10; $\beta_{med, Hif}$ = 0.66±0.04). A high correlation between regional β values from different states (r^2 = 0.91) indicated a similar topography for β regardless of brain states (**Figure 4C**).

4.5 The relationship between scaling parameters in calibrated fMRI

Figure 5 summarizes the relationship between the scaling parameters α, β, and M. With the same M value of 10%, the BOLD vs. CBF curves showed very different dependencies as β varied between 0.6 and 2. This implied that very different BOLD vs. CBF relationships could give rise to the same M value, which means M in the hypercapnic experiment would be estimated incorrectly if β was not independently measured for the subjects. The deviation could be smaller, however, for a lower α value (**Figure 5A**). For a typical visual stimulation in humans and somatosensory stimulation in rats at high fields, CMR_{O2} change was

calculated with calibrated fMRI for 1% and 4% BOLD signal change and with a fixed CBF change. While 1% BOLD signal change gave higher CMR_{O2} changes than 4% BOLD change, the difference is larger at higher β values (**Figure 5B**). Overall, these plots suggested that β has a significant impact on CMR_{O2} as calculated with calibrated fMRI.

5. DISCUSSION

Accurate quantification of CMR_{O2} with calibrated fMRI requires a number of scaling constants, such as β, to be pre-determined (see **Introduction**). Conventionally, in most human calibrated fMRI studies the assumed β value was 1.5 [R1.2] (Ances et al., 2008; Kastrup et al., 1999; Mohtasib et al., 2012; Restom et al., 2008; Stefanovic et al., 2004; Wey et al., 2011; Wu et al., 2002), but other β values between 0.9 and 2 have been proposed to account for factors such as field strengths, pulse sequence, and age of subjects (Boxerman et al., 1995; Bulte et al., 2009; Griffeth and Buxton, 2011; Kennan et al., 1994; Mark et al., 2011; Mohtasib et al., 2012; Wise et al., 2013). These β values were not measured in vivo, but approximated by numerical simulations. Since β describes the dependencies of the BOLD signal on deoxyhemoglobin-based susceptibility, using a singular β value demands that such dependencies are identical throughout the brain regardless of underlying physiological structures and/or neural activity levels. In this study these assumptions were examined. We mapped β *in vivo* across multiple regions in the white and gray matter and across different brain activity states by imaging R_2' (the difference between R_2* and R_2) as a function of contrast agent dosage **(Figure 1)**.

Besides separately measuring R_2* and R_2 to find R_2' (Shu et al., 2015), other methods have been developed in the past to measure R_2' in a single scan (Hyder et al., 2000b; Ma and Wehrli, 1996; Stables et al., 1998; Yablonskiy and Haacke, 1997). A recent study which compared these methods for human brain at 3.0T concluded that values of R_2' measured vary with the choice of methods, mainly because in each voxel signal decayed multi-exponentially rather than mono-exponentially. In such cases, β will depend on the technique used for measuring R_2' (Ni et al., 2015; Ulrich and Yablonskiy, 2015). At lower fields there is a significant relaxation component from the intravascular compartment, which could induce some multi-exponential behaviors to relaxations measured, specifically at lower spatial resolution. On the contrary, this study benefited from high magnetic field strength with its inherent higher spatial resolution and reduced intravascular weighting to achieve mono-exponential R_2' decay. Under these experimental conditions, R_2' and β should not vary significantly between R_2' methods, but further measurements are needed to confirm this [R1.1].

5.1 β values measured with different contrast agents

Though Molday and Feraheme share similar particle size (Wang et al., 2013), they are two distinctive forms of iron oxide-based contrast agents. The magnetite core of Molday is coated with dextran, whereas the magnetite core of Feraheme is coated with polyglucose sorbitol carboxymethyl ether to minimize immunological sensitivity (Pai and Garba, 2012). Balakrishnan et al. compared Feraheme to particles belonging to the iron dextran class and showed Feraheme had higher molecular weight but lower osmolality, and 5 min post-

injection in rats Feraheme had lower catalytic iron releases (Balakrishnan et al., 2009). Despite various physical differences between the two agents, we measured very similar β values **(Figure 2)**, as their post-injection changes in R_2, R_2*, and R_2' shared nearly identical trends. This suggests that the β mapping method can be applied for different contrast agents of similar particle size, provided that the nanoparticles have long circulation times. Because the fitting was based on relative increase in concentration of the agent, for human studies the dose of Feraheme can be flexibly designed to meet FDA regulation, where a total amount of 510 mg within three days is approved for adults (D'Arceuil et al., 2013).

5.2 β values measured across brain regions

In previous studies where an intravascular superparamagnetic contrast agent was injected, the increases in R_2 (ΔR_2) and R_2* (ΔR_2*) were related to the size of the vessels and blood volume fraction. At 2.35T, ΔR_2* was linearly proportional to blood volume fraction and ΔR_2 was linearly dependent on blood volume fraction but nonlinearly dependent on vessel size (Tropres et al., 2001). In our measurements at 9.4T, ΔR_2 was generally very small compared to ΔR_2*; additionally, ΔR_2 was uniform throughout the brain, whereas ΔR_2* (and therefore ΔR_2') was higher in superficial layers of the cortex **(Figure 1)**. Previous imaging studies showed that cortical microvessels are thinner in deeper layers (Lapi et al., 2008; Zhao et al., 2006), but despite the gradients observed in cortical ΔR_2' due to vessel size or blood volume fraction difference, β-values among all neocortical regions appeared homogeneous **(Figure 3)**, in contrast to former simulations and analyses (Boxerman et al., 1995; Ogawa et al., 1993; Yablonskiy and Haacke, 1994).

Given that the MRI contrast was obtained at 9.4T, there is minimal contributions from intravascular components. While the contrast induced by the iron oxide particles represent all vessels, the major contributions are likely to be from capillaries and venules as they together would represent nearly 80% of total vascular volume (Kim et al., 2006). It is possible, however, that the enhanced contrast in R_2' maps for higher dose of iron oxide particles could represent arterioles, given their superficial locations in the cortex. A difference between contrast generated by iron oxide and deoxyhemoglobin (i.e., intrinsic BOLD contrast) is that there will be relatively greater contrast at the venous end for BOLD due to higher susceptibility as a consequence of lower fractional oxygen binding to hemoglobin. However due to the extensive branching and convolutions of the vascular bed along with the high diffusivity of oxygen across walls of small blood vessels, there is an averaging of oxygen partial pressure across the venules and capillary beds which will considerably reduce heterogeneity. Thus the smoothness of β values in the cortex suggests relatively homogeneous coupling between metabolism and hemodynamics. However, further studies with vascular staining results are needed to confirm β's physiological dependence on vessel size across regions.

5.3 β values measured across brain states

β's dependency on brain states was examined with the use of α-chloralose and medetomidine anesthesia **(Figure 4)**. α-chloralose, as a GABAa receptor agonist, inhibits principle cells during resynchronization of the neural network (Garrett and Gan, 1998). Medetomidine is a α2-adrenoreceptor agonist which depresses mainly glutamate release and thereby causes

inhibition of excitatory glutamatergic transmission (Angenstein et al., 2010; Sinclair, 2003). To quantify the difference in neural activity between the two brain states induced by very different anesthetic mechanisms, MUA and LFP recordings were conducted separately for rats anesthesized with α-chloralose and medetomidine. The medetomidine group exhibited about a 100% increase in neural activity from α-chloralose **(Table 3)**, but R_2' (i.e., no contrast agent) in cortex varied just slightly with anesthesia **(Supplementary Figure 3)**. Given the linear relationship between neuronal activity and metabolic rates in mammalian brain (Hyder et al., 2013a), the R_2' change of about 10% in relation to neuronal activity or metabolic rates of about 100% observed in this 9.4T study is similar to observations by Kida et al at 7.0T (Kida et al., 2000). In this study, both the magnitude and pattern of β among the ROIs were very similar under both states, which suggests that β is not dependent on brain states. Therefore, the same β value should be applicable for subjects under different baseline brain activities, from being deeply anesthetized to being awake. However, β might vary with regional disease effects.

5.4 Implications for calibrated fMRI

As **eq. (9)** implies, determining the difference in CMR_{O2} between any two brain activity levels is subject to the scaling constants α, β, and M. The parameter α is the exponent in the power law relationship between CBF and CBV, describing how blood circulation impacts BOLD signal. The parameter β describes a hypothesized nonlinear BOLD signal dependence on magnetic susceptibility of blood, suggesting that deoxyhemoglobin has a weaker effect on BOLD signal change in smaller capillaries compared to larger veins due to the effects of diffusion (Kennan et al., 1994; Ogawa et al., 1993). Moreover, α and β play an important role in estimating M with the gas exposure technique, particularly with graded hypercapnia **(Figure 5A)** and during stimulation **(Figure 5B)**. Given the regional-dependent (van Raaij et al., 2012) and functionally dynamic (Kida et al., 2006) nature of α, measuring CBV directly instead of deriving it from CBF could improve the accuracy of M and CMR_{O2}.

With graded hypercapnia, simulations based on **eq. (8)** for the same sets of BOLD and CBF data (i.e., under isometabolic conditions) but different α and β values showed that there is an inverse relationship between β and M. With a typical α value of ~0.2, as β increases by a factor of three, M decreases equally by a factor of three. However with α value of ~0.4, M decreases by a factor of seven. **Eq. (8)** also suggested that with specific choices of β values, very different BOLD vs. CBF data can lead to the same M value **(Figure 5A)**. Thus, in graded hypercapnia values of M might be inaccurately estimated if α of 0.4 and β of 1.5 are assumed, unless very precise fitting is obtained for **eq. (8)** using high sensitivity calibrated fMRI data. The effects of α and β on M may further influence the accuracy of CMR_{O2} calculation, but the trend is dependent on the amplitude of BOLD (and CBF) change **(Figure 5B)**. CMR_{O2} differs by about 40% as β ranges between 0.6 and 2. Given the interdependence of these variables in **eq. (8)**, it is preferable to independently measure M with R_2' mapping (Shu et al., 2015) [R1.3].

Previously, Griffeth and Buxton provided a simulation approach for modeling the effects of various parameters on the Davis model for calibrated fMRI as depicted by **eq. (1)** (Davis et al., 1998), treating α and β as arbitrary fitting parameters devoid of physical meaning

(Griffeth and Buxton, 2011). According to their findings, the error in CMR_{O2} calculation for gray matter at 3T could effectively be minimized if M was perfectly estimated with α and β values of 0.14 and 0.91, respectively. At higher magnetic field strengths, as the BOLD signal becomes increasingly extravascular (Donahue et al., 2011; Duong et al., 2003; Silvennoinen et al., 2003), and it was argued, based on simulations, that β value should be reduced (Boxerman et al., 1995; Bulte et al., 2009; Kennan et al., 1994; Mark et al., 2011; Ogawa et al., 1993). In accordance with this, earlier high field calibrated fMRI studies have assumed β value to be 1 (Herman et al., 2013; Hyder et al., 2001; Kida et al., 2000). In this study at 9.4T we obtained β values of ~0.8 in the cortex and thus verified experimentally that cortical β values are less than 1.5 at high fields, but further measurements are necessary to characterize β values across different magnetic fields.

In the white matter and subcortical gray matter regions β values were ~0.6. Also, much greater extent of heterogeneity was found in subcortical gray matter than in white matter. Recently there has been emerging interest in studying BOLD contrast in white matter as a potential marker for diagnosing white matter connectivity disorders, but the exact mechanism contributing to the BOLD signal in white matter is still not fully understood (Gawryluk et al., 2014). Measuring β in corpus callosum, fimbria fornix, and internal capsule can bring insights to the neurovascular and neurometabolic coupling underlying the BOLD signal in white matter.

6. SUMMARY

This study demonstrated a method to map β *in vivo* for the whole brain. Our results suggest that β values range between 0.5 and 1.0 in the rodent brain, with the cortical gray matter regions being uniformly higher than the subcortical gray matter and white matter regions. The source of difference between our cortical β value of 0.8 vs. the commonly adopted 1.5 across different magnetic fields is a topic for future studies. A measured β map per subject scanned will allow more accurate calculations of CMR_{O2} with calibrated fMRI. Since the dosages used in this study would be compatible for human subjects using an approved contrast agent, this method can be readily applied to human studies.

Supplementary Material

Refer to Web version on PubMed Central for supplementary material.

ACKNOWLEDGEMENT

Thanks to Xenophon Papademetris for inputs on image analysis software and Bei Wang for assistance in animal surgeries. Supported by NIH grants (R01 MH-067528, R01 AG-034953, P30 NS-052519).

REFERENCES

Ances BM, Leontiev O, Perthen JE, Liang C, Lansing AE, Buxton RB. Regional differences in the coupling of cerebral blood flow and oxygen metabolism changes in response to activation: implications for BOLD-fMRI. Neuroimage. 2008; 39:1510–1521. [PubMed: 18164629]

Angenstein F, Krautwald K, Scheich H. The current functional state of local neuronal circuits controls the magnitude of a BOLD response to incoming stimuli. Neuroimage. 2010; 50:1364–1375. [PubMed: 20114080]

Balakrishnan VS, Rao M, Kausz AT, Brenner L, Pereira BJ, Frigo TB, Lewis JM. Physicochemical properties of ferumoxytol, a new intravenous iron preparation. Eur J Clin Invest. 2009; 39:489–496. [PubMed: 19397688]

Blockley NP, Griffeth VE, Simon AB, Dubowitz DJ, Buxton RB. Calibrating the BOLD response without administering gases: Comparison of hypercapnia calibration with calibration using an asymmetric spin echo. Neuroimage. 2015; 104:423–429. [PubMed: 25451475]

Boxerman JL, Hamberg LM, Rosen BR, Weisskoff RM. MR contrast due to intravascular magnetic susceptibility perturbations. Magn Reson Med. 1995; 34:555–566. [PubMed: 8524024]

Bulte DP, Drescher K, Jezzard P. Comparison of hypercapnia-based calibration techniques for measurement of cerebral oxygen metabolism with MRI. Magnetic Resonance in Medicine. 2009; 61:391–398. [PubMed: 19165902]

Buxton RB, Uludag K, Dubowitz DJ, Liu TT. Modeling the hemodynamic response to brain activation. Neuroimage 23 Suppl. 2004; 1:S220–233.

Calabrese E, Badea A, Watson C, Johnson GA. A quantitative magnetic resonance histology atlas of postnatal rat brain development with regional estimates of growth and variability. Neuroimage. 2013; 71:196–206. [PubMed: 23353030]

Christen T, Ni W, Qiu D, Schmiedeskamp H, Bammer R, Moseley M, Zaharchuk G. High-resolution cerebral blood volume imaging in humans using the blood pool contrast agent ferumoxytol. Magn Reson Med. 2013; 70:705–710. [PubMed: 23001902]

Christen T, Pannetier NA, Ni WW, Qiu D, Moseley ME, Schuff N, Zaharchuk G. MR vascular fingerprinting: A new approach to compute cerebral blood volume, mean vessel radius, and oxygenation maps in the human brain. Neuroimage. 2014; 89:262–270. [PubMed: 24321559]

D'Arceuil H, Coimbra A, Triano P, Dougherty M, Mello J, Moseley M, Glover G, Lansberg M, Blankenberg F. Ferumoxytol enhanced resting state fMRI and relative cerebral blood volume mapping in normal human brain. Neuroimage. 2013; 83:200–209. [PubMed: 23831413]

Davis TL, Kwong KK, Weisskoff RM, Rosen BR. Calibrated functional MRI: mapping the dynamics of oxidative metabolism. Proc Natl Acad Sci U S A. 1998; 95:1834–1839. [PubMed: 9465103]

Donahue MJ, Hoogduin H, van Zijl PC, Jezzard P, Luijten PR, Hendrikse J. Blood oxygenation level-dependent (BOLD) total and extravascular signal changes and DeltaR2* in human visual cortex at 1.5, 3.0 and 7.0 T. NMR Biomed. 2011; 24:25–34. [PubMed: 21259367]

Duong TQ, Yacoub E, Adriany G, Hu X, Ugurbil K, Kim SG. Microvascular BOLD contribution at 4 and 7 T in the human brain: gradient-echo and spin-echo fMRI with suppression of blood effects. Magn Reson Med. 2003; 49:1019–1027. [PubMed: 12768579]

Fujita N, Shinohara M, Tanaka H, Yutani K, Nakamura H, Murase K. Quantitative mapping of cerebral deoxyhemoglobin content using MR imaging. Neuroimage. 2003; 20:2071–2083. [PubMed: 14683711]

Garrett KM, Gan J. Enhancement of gamma-aminobutyric acidA receptor activity by alpha-chloralose. J Pharmacol Exp Ther. 1998; 285:680–686. [PubMed: 9580613]

Gati JS, Menon RS, Ugurbil K, Rutt BK. Experimental determination of the BOLD field strength dependence in vessels and tissue. Magn Reson Med. 1997; 38:296–302. [PubMed: 9256111]

Gawryluk JR, Mazerolle EL, D'Arcy RC. Does functional MRI detect activation in white matter? A review of emerging evidence, issues, and future directions. Front Neurosci. 2014; 8:239. [PubMed: 25152709]

Griffeth VE, Buxton RB. A theoretical framework for estimating cerebral oxygen metabolism changes using the calibrated-BOLD method: modeling the effects of blood volume distribution, hematocrit, oxygen extraction fraction, and tissue signal properties on the BOLD signal. Neuroimage. 2011; 58:198–212. [PubMed: 21669292]

Grubb RL Jr. Raichle ME, Eichling JO, Ter-Pogossian MM. The effects of changes in PaCO2 on cerebral blood volume, blood flow, and vascular mean transit time. Stroke. 1974; 5:630–639. [PubMed: 4472361]

Herman P, Sanganahalli BG, Blumenfeld H, Rothman DL, Hyder F. Quantitative basis for neuroimaging of cortical laminae with calibrated functional MRI. Proc Natl Acad Sci U S A. 2013; 110:15115–15120. [PubMed: 23980158]

Hoge RD. Calibrated FMRI. Neuroimage. 2012; 62:930–937. [PubMed: 22369993]

Hoge RD, Atkinson J, Gill B, Crelier GR, Marrett S, Pike GB. Investigation of BOLD signal dependence on cerebral blood flow and oxygen consumption: the deoxyhemoglobin dilution model. Magn Reson Med. 1999; 42:849–863. [PubMed: 10542343]

Hyder F, Fulbright RK, Shulman RG, Rothman DL. Glutamatergic function in the resting awake human brain is supported by uniformly high oxidative energy. J Cereb Blood Flow Metab. 2013a; 33:339–347. [PubMed: 23299240]

Hyder F, Kennan RP, Kida I, Mason GF, Behar KL, Rothman D. Dependence of oxygen delivery on blood flow in rat brain: a 7 tesla nuclear magnetic resonance study. J Cereb Blood Flow Metab. 2000a; 20:485–498. [PubMed: 10724113]

Hyder F, Kida I, Behar KL, Kennan RP, Maciejewski PK, Rothman DL. Quantitative functional imaging of the brain: towards mapping neuronal activity by BOLD fMRI. NMR Biomed. 2001; 14:413–431. [PubMed: 11746934]

Hyder F, Renken R, Kennan RP, Rothman DL. Quantitative multi-modal functional MRI with blood oxygenation level dependent exponential decays adjusted for flow attenuated inversion recovery (BOLDED AFFAIR). Magnetic Resonance Imaging. 2000b; 18:227–235. [PubMed: 10745130]

Hyder F, Rothman DL. Quantitative fMRI and oxidative neuroenergetics. Neuroimage. 2012; 62:985–994. [PubMed: 22542993]

Hyder, F.; Shu, CY.; Herman, P.; Sanganahalli, BG.; Coman, D.; Rothman, DL. Quantifying morphology and physiology of the human body using MRI.. In: Muftuler, LT., editor. Series in medical physics and biomedical engineering. CRC Press/Taylor & Francis Group; Boca Raton, FL: 2013b. p. 99-124.

Juchem C, Herman P, Sanganahalli BG, Brown PB, McIntyre S, Nixon TW, Green D, Hyder F, de Graaf RA. DYNAmic Multi-coIl TEchnique (DYNAMITE) shimming of the rat brain at 11.7 T. NMR Biomed. 2014; 27:897–906. [PubMed: 24839167]

Kastrup A, Kruger G, Glover GH, Moseley ME. Assessment of cerebral oxidative metabolism with breath holding and fMRI. Magn Reson Med. 1999; 42:608–611. [PubMed: 10467308]

Kennan RP, Zhong J, Gore JC. Intravascular susceptibility contrast mechanisms in tissues. Magn Reson Med. 1994; 31:9–21. [PubMed: 8121277]

Kida I, Kennan RP, Rothman DL, Behar KL, Hyder F. High-resolution CMR(O2) mapping in rat cortex: a multiparametric approach to calibration of BOLD image contrast at 7 Tesla. J Cereb Blood Flow Metab. 2000; 20:847–860. [PubMed: 10826536]

Kida I, Rothman DL, Hyder F. Dynamics of changes in blood flow, volume, and oxygenation: implications for dynamic functional magnetic resonance imaging calibration. J Cereb Blood Flow Metab. 2006; 27:690–696. [PubMed: 17033688]

Kim S-G, Harel N, Jin T, Kim T, Lee P, Zhao F. Cerebral blood volume MRI with intravascular superparamagnetic iron oxide nanoparticles. NMR Biomed. 2013; 26:949–962. [PubMed: 23208650]

Kim T, Hendrich KS, Masamoto K, Kim S-G. Arterial versus total blood volume changes during neural activity-induced cerebral blood flow change: implication for BOLD fMRI. J Cereb Blood Flow Metab. 2006; 27:1235–1247. [PubMed: 17180136]

Lapi D, Marchiafava PL, Colantuoni A. Geometric characteristics of arterial network of rat pial microcirculation. J Vasc Res. 2008; 45:69–77. [PubMed: 17901708]

Ma J, Wehrli FW. Method for image-based measurement of the reversible and irreversible contribution to the transverse-relaxation rate. J Magn Reson B. 1996; 111:61–69. [PubMed: 8620286]

Mark CI, Fisher JA, Pike GB. Improved fMRI calibration: Precisely controlled hyperoxic versus hypercapnic stimuli. Neuroimage. 2011; 54:1102–1111. [PubMed: 20828623]

Mohtasib RS, Lumley G, Goodwin JA, Emsley HC, Sluming V, Parkes LM. Calibrated fMRI during a cognitive Stroop task reveals reduced metabolic response with increasing age. Neuroimage. 2012; 59:1143–1151. [PubMed: 21843646]

Ni W, Christen T, Zun Z, Zaharchuk G. Comparison of R2' measurement methods in the normal brain at 3 Tesla. Magn Reson Med. 2015; 73:1228–1236. [PubMed: 24753286]

Ogawa S, Menon RS, Tank DW, Kim SG, Merkle H, Ellermann JM, Ugurbil K. Functional brain mapping by blood oxygenation level-dependent contrast magnetic resonance imaging. A

comparison of signal characteristics with a biophysical model. Biophys J. 1993; 64:803–812. [PubMed: 8386018]

Pai AB, Garba AO. Ferumoxytol: a silver lining in the treatment of anemia of chronic kidney disease or another dark cloud? J Blood Med. 2012; 3:77–85. [PubMed: 22973119]

Papademetris X, Jackowski MP, Rajeevan N, DiStasio M, Okuda H, Constable RT, Staib LH. BioImage Suite: An integrated medical image analysis suite: An update. Insight J. 2006; 2006:209. [PubMed: 25364771]

Pawela CP, Biswal BB, Hudetz AG, Schulte ML, Li R, Jones SR, Cho YR, Matloub HS, Hyde JS. A protocol for use of medetomidine anesthesia in rats for extended studies using task-induced BOLD contrast and resting-state functional connectivity. Neuroimage. 2009; 46:1137–1147. [PubMed: 19285560]

Restom K, Perthen JE, Liu TT. Calibrated fMRI in the medial temporal lobe during a memory-encoding task. Neuroimage. 2008; 40:1495–1502. [PubMed: 18329291]

Shu CY, Herman P, Coman D, Sanganahalli BG, Wang H, Juchem C, Rothman DL, de Graaf RA, Hyder F. Brain region and activity-dependent properties of M for calibrated fMRI. Neuroimage. 2015

Silva AC, Lee SP, Yang G, Iadecola C, Kim SG. Simultaneous blood oxygenation level-dependent and cerebral blood flow functional magnetic resonance imaging during forepaw stimulation in the rat. J Cereb Blood Flow Metab. 1999; 19:871–879. [PubMed: 10458594]

Silvennoinen MJ, Clingman CS, Golay X, Kauppinen RA, van Zijl PC. Comparison of the dependence of blood R2 and R2* on oxygen saturation at 1.5 and 4.7 Tesla. Magn Reson Med. 2003; 49:47–60. [PubMed: 12509819]

Sinclair MD. A review of the physiological effects of alpha2-agonists related to the clinical use of medetomidine in small animal practice. Can Vet J. 2003; 44:885–897. [PubMed: 14664351]

Stables LA, Kennan RP, Gore JC. Asymmetric spin-echo imaging of magnetically inhomogeneous systems: theory, experiment, and numerical studies. Magn Reson Med. 1998; 40:432–442. [PubMed: 9727947]

Stefanovic B, Warnking JM, Pike GB. Hemodynamic and metabolic responses to neuronal inhibition. Neuroimage. 2004; 22:771–778. [PubMed: 15193606]

Tropres I, Grimault S, Vaeth A, Grillon E, Julien C, Payen JF, Lamalle L, Decorps M. Vessel size imaging. Magn Reson Med. 2001; 45:397–408. [PubMed: 11241696]

Ulrich X, Yablonskiy DA. Separation of cellular and BOLD contributions to T2* signal relaxation. Magnetic Resonance in Medicine. 2015 n/a-n/a.

van Raaij ME, Lindvere L, Dorr A, He J, Sahota B, Foster FS, Stefanovic B. Quantification of blood flow and volume in arterioles and venules of the rat cerebral cortex using functional micro-ultrasound. Neuroimage. 2012; 63:1030–1037. [PubMed: 22871388]

Wang Y-XJ. Superparamagnetic iron oxide based MRI contrast agents: Current status of clinical application. Quantitative Imaging in Medicine and Surgery. 2011; 1:35–40. [PubMed: 23256052]

Wang Y, Xu C, Ow H. Commercial nanoparticles for stem cell labeling and tracking. Theranostics. 2013; 3:544–560. [PubMed: 23946821]

Wey HY, Wang DJ, Duong TQ. Baseline CBF, and BOLD, CBF, and CMRO2 fMRI of visual and vibrotactile stimulations in baboons. J Cereb Blood Flow Metab. 2011; 31:715–724. [PubMed: 20827260]

Wise RG, Harris AD, Stone AJ, Murphy K. Measurement of OEF and absolute CMRO2: MRI-based methods using interleaved and combined hypercapnia and hyperoxia. Neuroimage. 2013; 83:135–147. [PubMed: 23769703]

Wu G, Luo F, Li Z, Zhao X, Li SJ. Transient relationships among BOLD, CBV, and CBF changes in rat brain as detected by functional MRI. Magn Reson Med. 2002; 48:987–993. [PubMed: 12465108]

Yablonskiy DA, Haacke EM. Theory of NMR signal behavior in magnetically inhomogeneous tissues: the static dephasing regime. Magn Reson Med. 1994; 32:749–763. [PubMed: 7869897]

Yablonskiy DA, Haacke EM. An MRI method for measuring T2 in the presence of static and RF magnetic field inhomogeneities. Magn Reson Med. 1997; 37:872–876. [PubMed: 9178238]

Zhao F, Wang P, Hendrich K, Ugurbil K, Kim SG. Cortical layer-dependent BOLD and CBV responses measured by spin-echo and gradient-echo fMRI: insights into hemodynamic regulation. Neuroimage. 2006; 30:1149–1160. [PubMed: 16414284]

Highlights

- β reflects the dependence between BOLD signal and deoxyhemoglobin concentration.
- A method to map β in vivo for the whole brain is demonstrated.
- β is measured to be uniformly 0.8 within the neocortex, significantly lower than the previously assumed value of 1.5.
- As resting brain activity level is varied with different anesthesia, β does not change significantly.
- The impact of measured β values on calibrated fMRI is discussed.

ARTWORKS WITH CAPTIONS

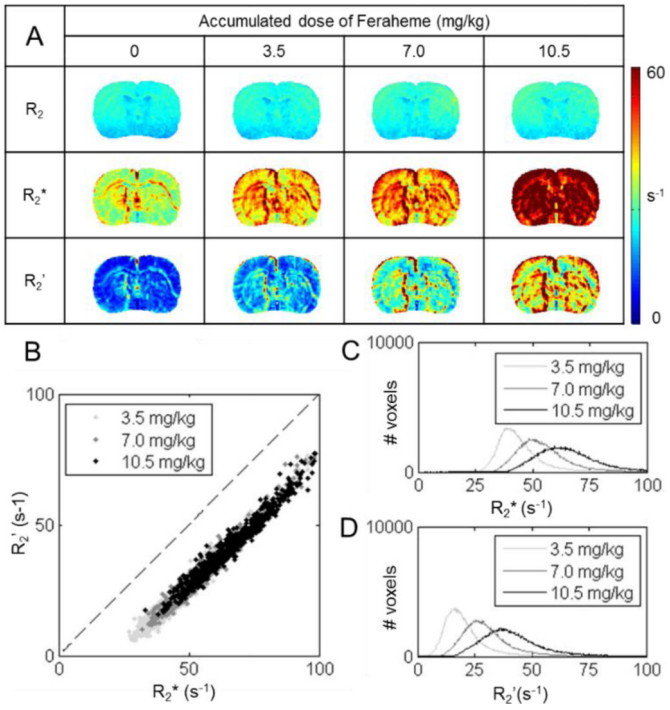

Figure 1.

A summary of relaxation rates measured with Feraheme (under α-chloralose). Images shown are from a representative slice for a single subject. (A) R_2(top), R_2* (middle), and R_2' (bottom) were measured prior to and after each dose (i.e., 3.5 mg/kg) of Feraheme. As more Feraheme was present in the blood, R_2, R_2*, and R_2' all increased, though the trend is more obvious for R_2* and R_2' than for R_2. (B) Summary on the relationship between R_2* and R_2' across different concentrations of Feraheme. A very strong correlation was observed ($r^2 = 0.95$). (C, D) Distributions of whole brain R_2* (C) and R_2' (D), measured after each dose of Feraheme was injected. Both R_2* and R_2' shifted higher with higher concentration of Feraheme in the blood. Based on the single slice shown in this figure, β fitted according to **eq. (7)** by R_2 and R_2* (0.07±0.04 and 0.36±0.10) maps were much lower compared to β fitted by R_2' maps (0.66±0.20).

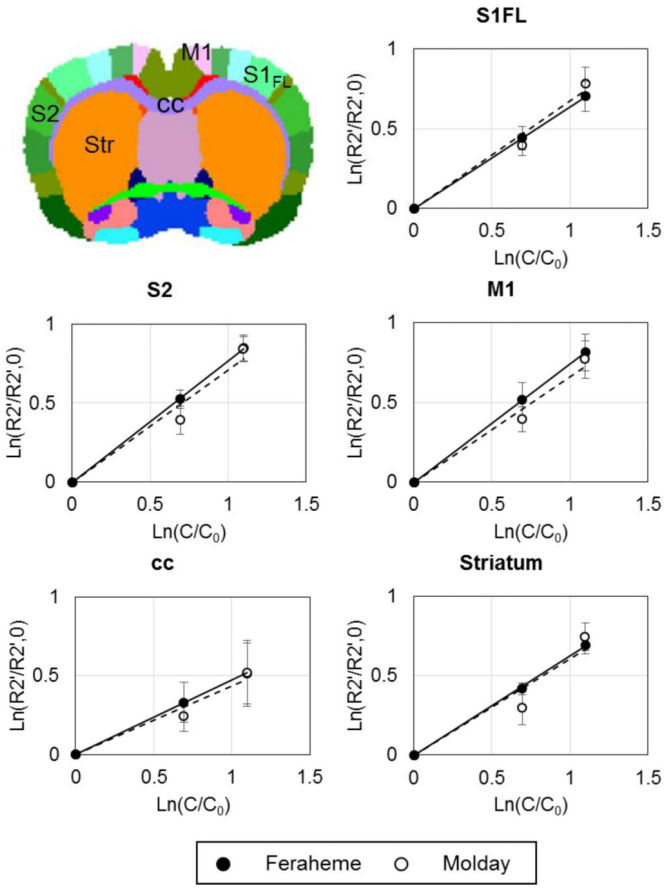

Figure 2.

Comparison of β measured with Molday vs. Feraheme in various ROIs (under α-chloralose) with mean and SD values. In the vertical axis, R_2' measured after each dose of contrast agent were divided by R_2' measured after the first dose. Similarly, in the horizontal axis amount of accumulated doses were divided by the first dose. Their relationships were linearized to fit for β. See also **Table 2** for each individual R_2' values. Fitting R_2' and concentration of contrast agent (i.e., c, where c_0 stands for initial concentration) according to **eq. (7)** in various ROIs of the brain gave similar slopes (i.e., β) between Molday and Feraheme. β with Feraheme was 0.63 in $S1_{FL}$, 0.52 in cc, 0.73 in M1, 0.76 in S2, and 0.62 in Str; β with Molday was 0.68 in $S1_{FL}$, 0.49 in cc, 0.75 in M1, 0.71 in S2 and 0.59 in Str. The r^2 for the correlations were from 0.92 to 0.99, suggesting strong linear relationships.

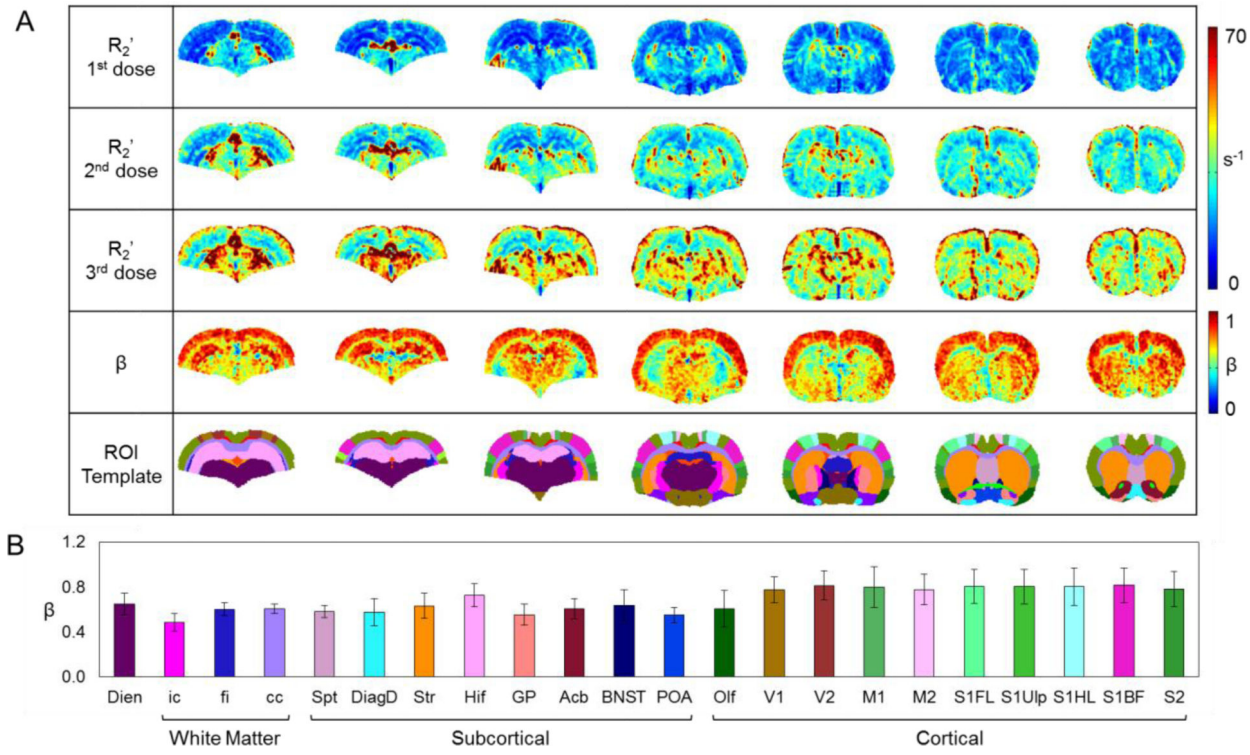

Figure 3.

A summary of dose-dependent R_2' and the mean β in each ROI (under α-chloralose). (A) R_2' images for the same subject after one, two, and three doses of Feraheme by which β was fitted. Cortical gray matter showed uniformly higher β compared to other regions. (B) An atlas was used to calculate mean and SDs of β across 22 ROIs. Consistent with the images, the mean β was 0.78 among the cortical gray matter regions, 0.56 in the white matter, and 0.61 in the subcortex.

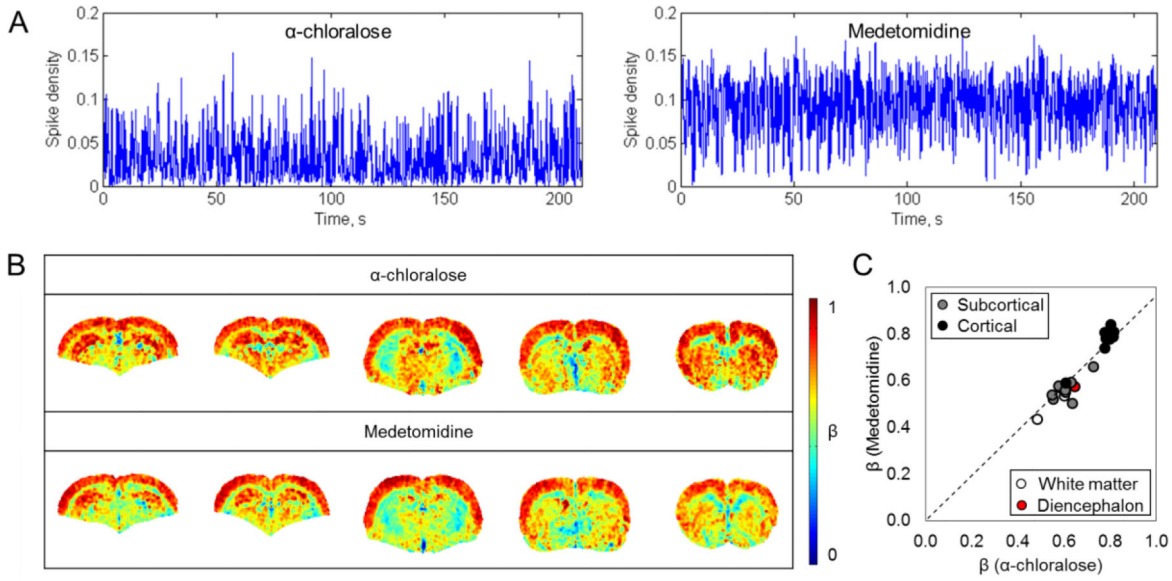

Figure 4.

Comparison between β measured at different brain activity levels (α-chloralose vs. medetomidine). (A) A comparison of the corresponding spike density functions showed a roughly two times higher activity level with medetomidine. See also **Table 3**. (B) Mean β images for representative slices in rats anesthetized with α-chloralose and medetomidine. (C) Relationship between regional β with α-chloralose (β_α) and medetomidine (β_{med}) showed strong correlation ($r^2 = 0.91$), indicating a very similar pattern for β in all ROIs across brain states. Regions of both maximum and minimum for β were nearly identical among α-chloralose and medetomidine. Among all ROIs, maximum β was among the primary somatosensory regions, while minimum β was found in ic ($B_\alpha = 0.48\pm0.08$. $\beta_{med} = 0.43\pm0.01$). In subcortical gray matter, maximum β was observed in Hif ($B_\alpha = 0.73\pm0.10$. $\beta_{med} = 0.66\pm0.04$). ANOVA test suggested that β_{med} were not significantly different from β_α ($p > 0.05$). Likewise, student's t-test did not give significant difference in any ROI between α-chloralose and medetomidine.

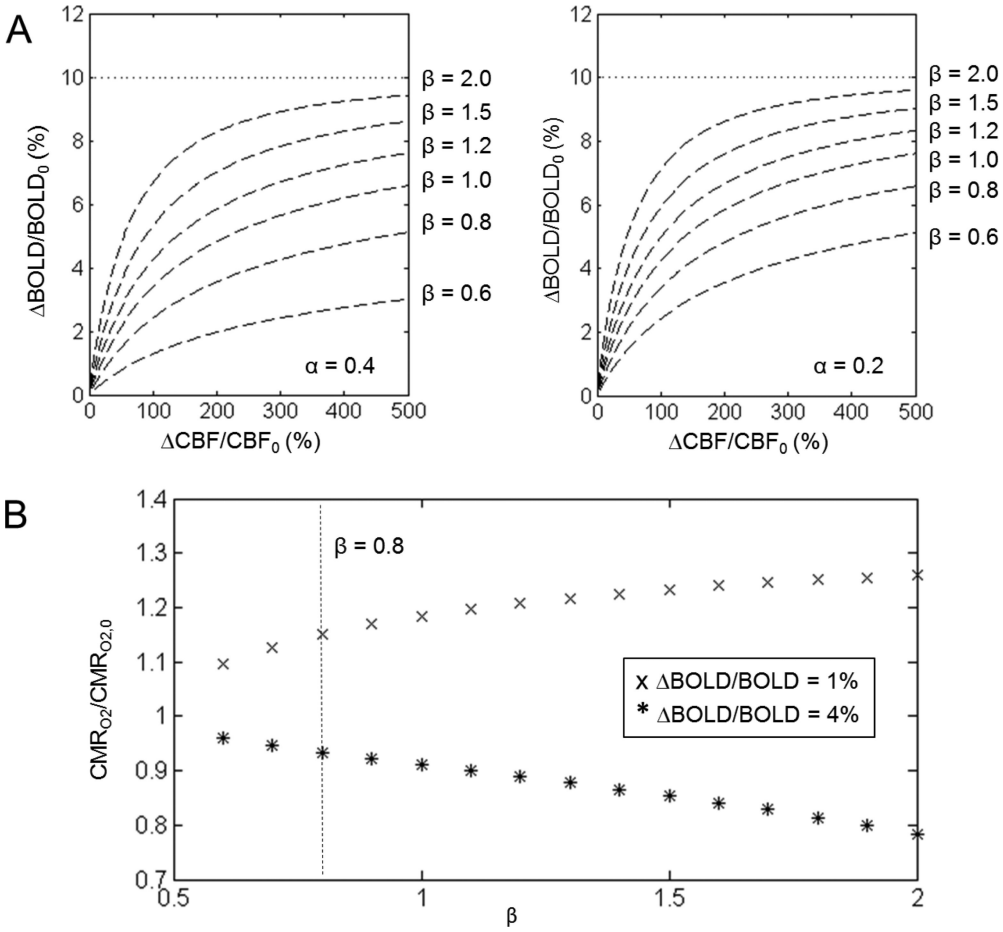

Figure 5.

The relationships between α, M, and CMR_{O2} change for calibrated fMRI (see **eqs. (1) and (8)**). (A) Fractional change of BOLD vs CBF during graded hypercapnia for a fixed value of M behaves differently for different values of α and β. The value of M was determined from an assumed asymptotic relationship with measured BOLD and CBF changes. Thus M would be estimated incorrectly if an inaccurate β value was used in the hypercapnic experiment, but the discrepancy is smaller for a lower α value. (B) CMR_{O2} change calculated from **eq. (9)** based on $\Delta BOLD/BOLD_0$ and CBF/CBF_0 typically observed during a somatosensory stimulation in rats (4% ΔBOLD/BOLD) and a visual stimulation in humans (1% ΔBOLD/BOLD) (Donahue et al., 2011; Herman et al., 2013; Silva et al., 1999). For 1% change in the BOLD signal, higher β values resulted in higher $CMR_{O2}/CMR_{O2,0}$ estimation, but the trend is opposite for 4% change in the BOLD signal. The dotted vertical line represents the β value of 0.8.

Table 1

Physiological parameters during experiments.

Physiological Parameters	α-chloralose	Medetomidine
pH	7.3±0.0	7.4±0.0
pO2 (mmHg)	115±12	99.5±19
pCO2 (mmHg)	40±2.6	41±0.6
Blood pressure (mmHg)	119±14	118±18

Table 2

R_2' (mean±SD) measured in different regions of the brain after each dose of Molday or Feraheme. See also **Figure 2.**

dose	R_2' in S1FL (s^{-1})		R_2' in cc (s^{-1})		R_2' in M1 (s^{-1})		R_2' in Str (s^{-1})		R_2' in S2 (s^{-1})	
	Molday	Feraheme	Molday	Feraheme	Molday	Feraheme	Molday	Feraheme	Molday	Feraheme
1st dose	39.7±5.3	22.1±5.4	44.4±5.7	17.9±3.8	42.7±8.2	17.1±2.6	57.8±15.0	29.8±6.4	47.1±7.2	20.4±4.6
2nd dose	58.9±7.7	34.3±8.6	58.5±8.1	25.9±4.3	65.7±14.0	29.0±5.4	77.0±11.9	45.3±9.2	70.1±15.6	34.5±8.0
3rd dose	87.3±14.4	44.3±9.2	79.7±10.5	31.8±3.8	99.9±28.8	38.8±7.7	119.6±22.1	59.0±12.0	109.5±19.8	46.8±7.8

Table 3

Root mean square (RMS) of LFP amplitude (mean±SD) and the spike rate (mean±SD) from MUA recordings for α-chloralose and medetomidine. See also Figure 4.

Electrophysiological recordings	α-chloralose	medetomidine
RMS	1.3±0.1	3.0±0.7
Spike rate (Hz)	4.2±1.1	7.3±1.1